

XAS Opportunities for Geological and High Pressure Science



Wendy L. Mao

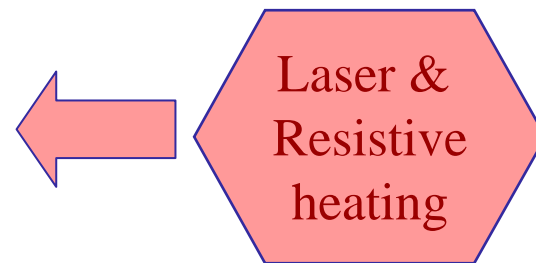
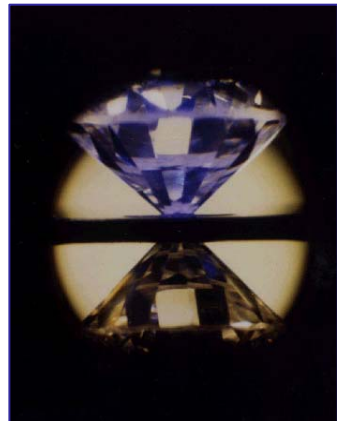
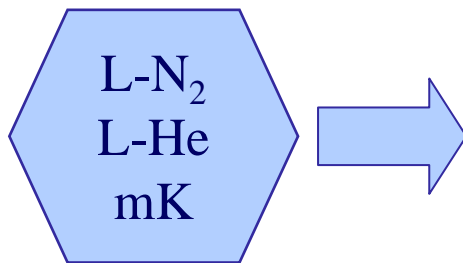
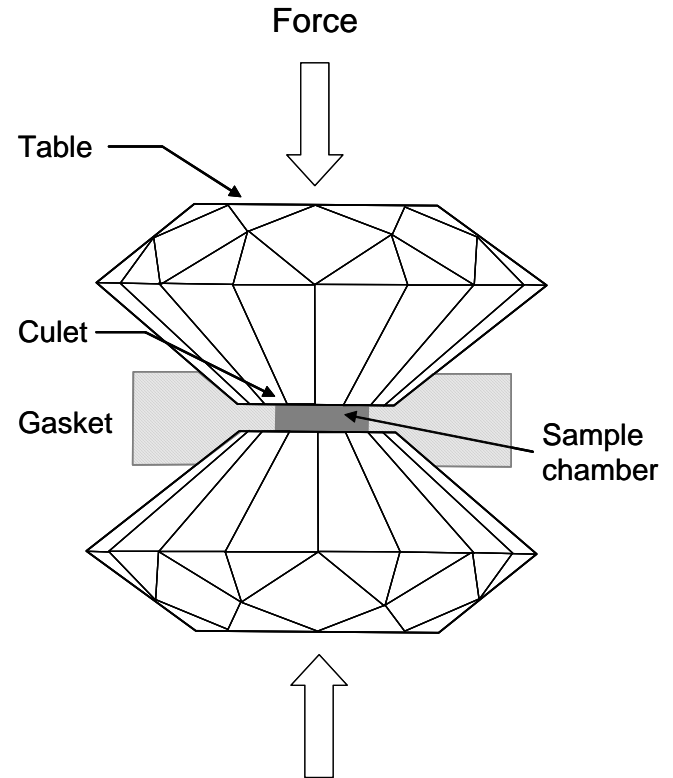
*Geological and Environmental Sciences &
Photon Science, SSRL, Stanford University*

Outline

- High pressure studies
 - Diamond anvil cell
 - Ex. Fe in the deep Earth
- What can XAS at high pressure tell us?
 - XAS in DAC
 - Ex. Fe in the deep Earth
 - Other examples enabled by NSLS-II

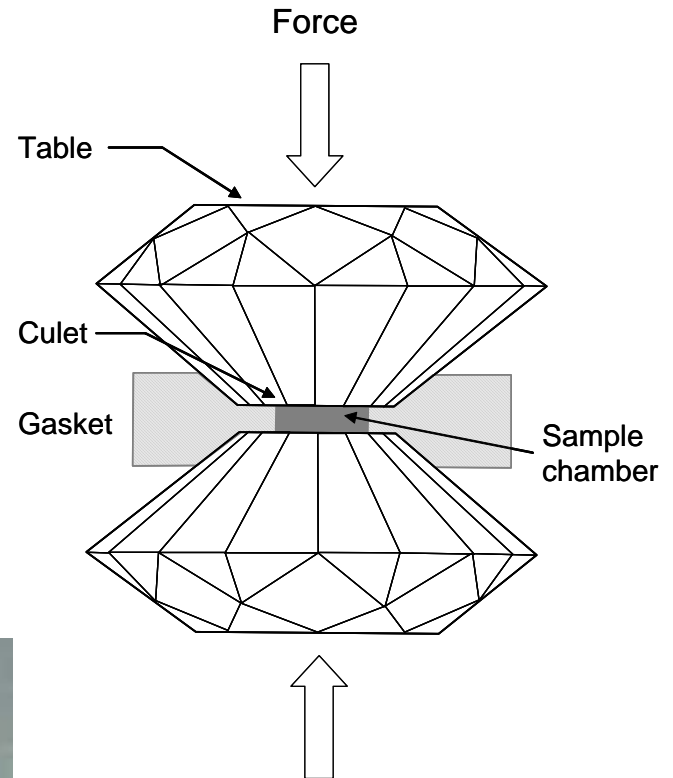
How do we study materials at high pressure?

- Diamond Anvil Cell (DAC)
 - Pressure: ambient to 500 GPa (1 GPa= 10,000 bar)
 - Temp: mK to 5000 K
 - Sample size: $< 0.001 \text{ mm}^3$
 - Transparent to large range of E-M radiation

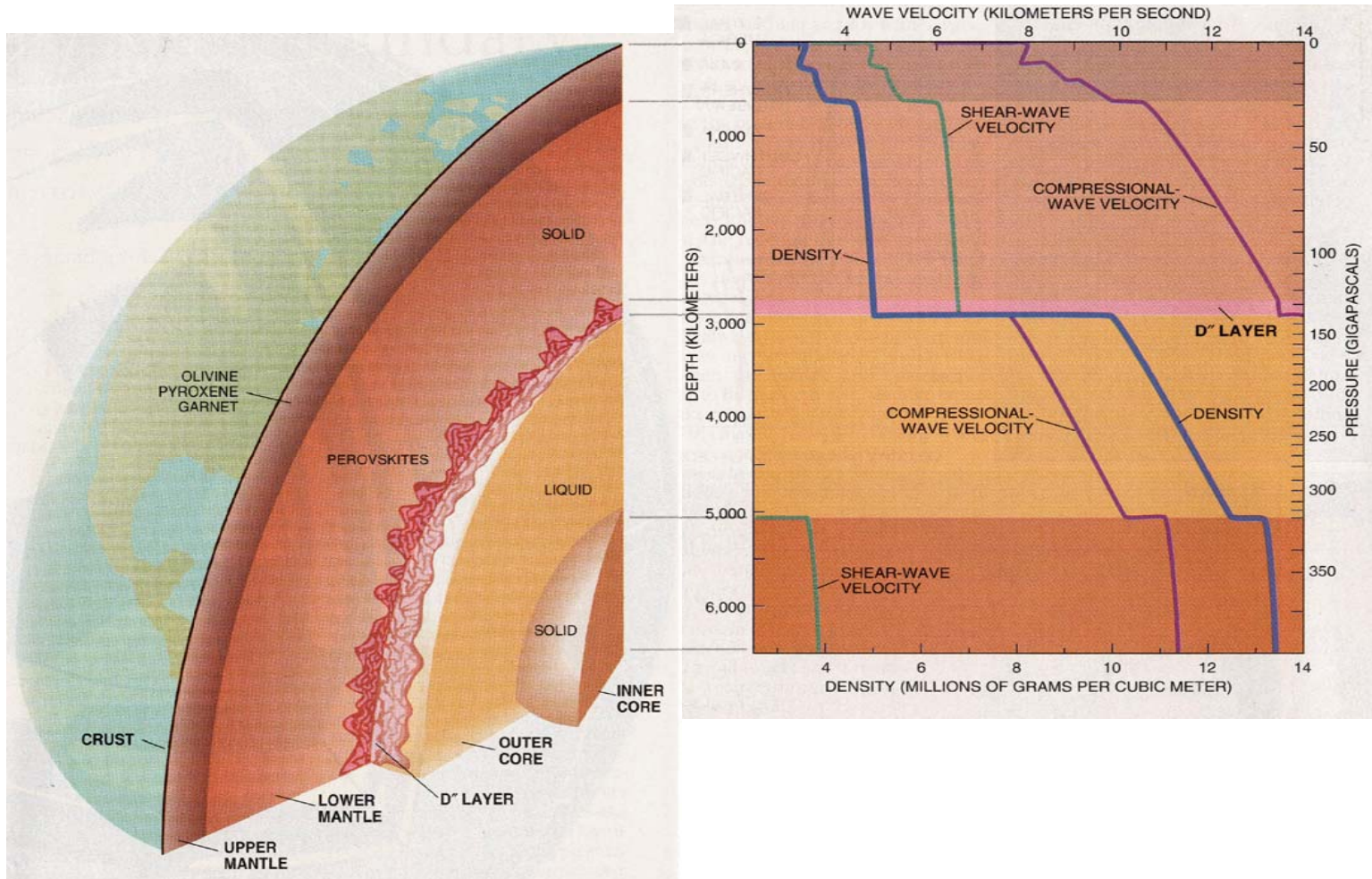


How do we study materials at high pressure?

- Diamond Anvil Cell (DAC)
 - Pressure: ambient to 500 GPa (1 GPa= 10,000 bar)
 - Temp: mK to 5000 K
 - Sample size: $< 0.001 \text{ mm}^3$
 - Transparent to large range of E-M radiation



Understanding the Earth's interior

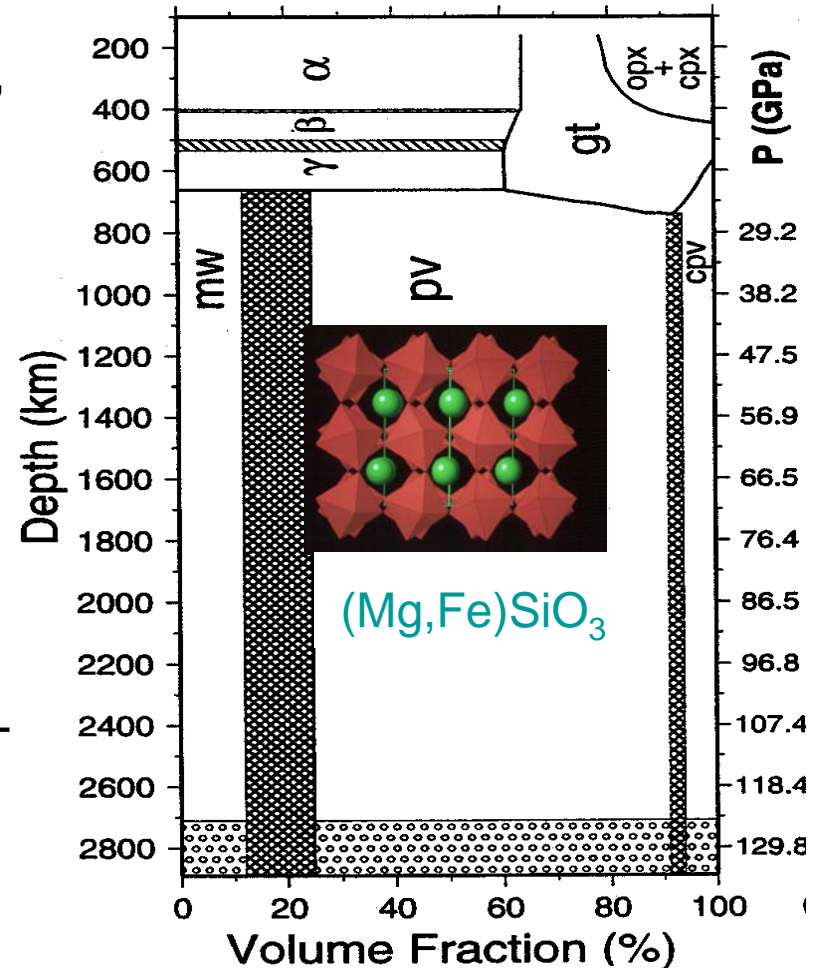


“The interior of the Earth is a problem at once fascinating and baffling, as one may easily judge from the vast literature, and the few established facts, concerning it.”

- Francis Birch (1952)

Fe in the deep Earth

- Fe is the most abundant element by wt, most important transition element
- Complex speciation
 - Oxidation state (Fe^0 , Fe^{2+} , Fe^{3+})
 - Coordination (4, 5, 6, 8)
- Fe distribution and speciation between melt and among different crystalline phases (ol, px, wad, ringwoodite, pv, ppv, mw, etc.) throughout the mantle is a central solid-Earth question
 - controls the evolution of the Earth, core-mantle differentiation, and the geodynamics of the mantle.
 - Different P-T-x for different regions and geologic time



Ringwood, *Composition and Petrology of the Earth's Mantle* (1975)

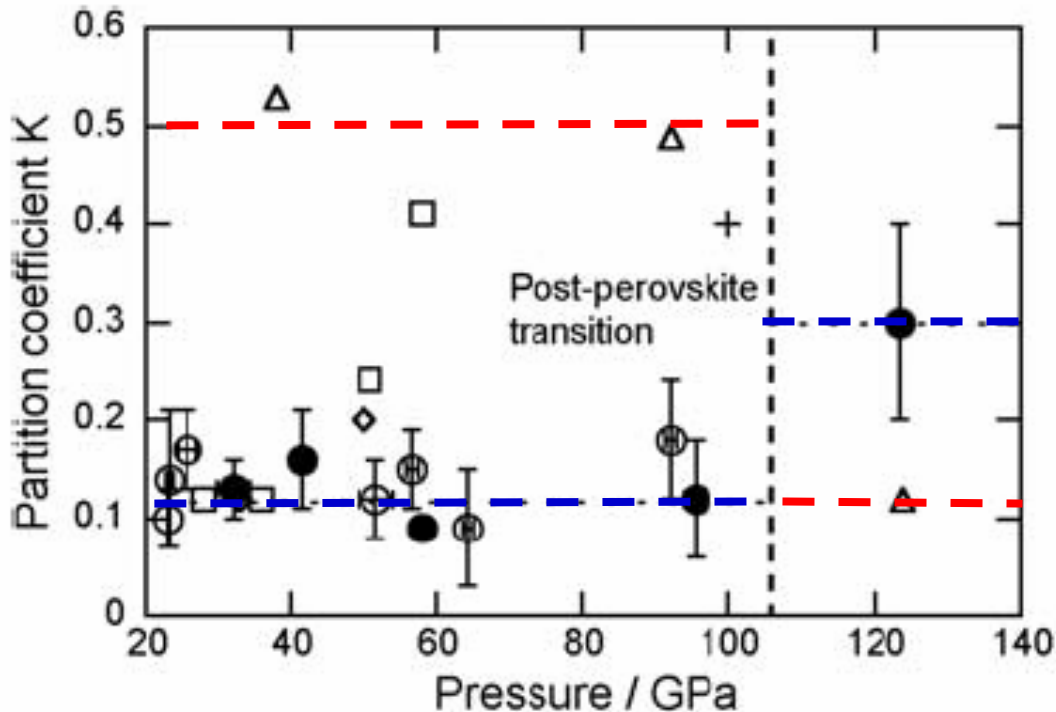
Bina, *Ultrahigh Pressure Mineralogy* (1998)

Fe in the deep Earth

- Our knowledge of Fe distribution relies on understanding the drastic changes in the physical and chemical properties of Fe species at extreme P - T conditions:
 - Fe/Mg partitioning
 - Fe/Mg diffusion
 - Fe speciation in solid and liquid
 - Fe redox
 - Electronic spin state (high-intermediate-low)

Fe-Mg partitioning

$$K = \frac{(Fe/Mg)_{silicate}}{(Fe/Mg)_{mw}} \quad \begin{array}{l} (Mg,Fe)SiO_3 \\ (Mg,Fe)O \end{array}$$



◇ Mao *et al*, *Science* 1997

□ Andrault *et al*, *JGR* 2001

+ Kessen *et al*, *EPSL* 2002

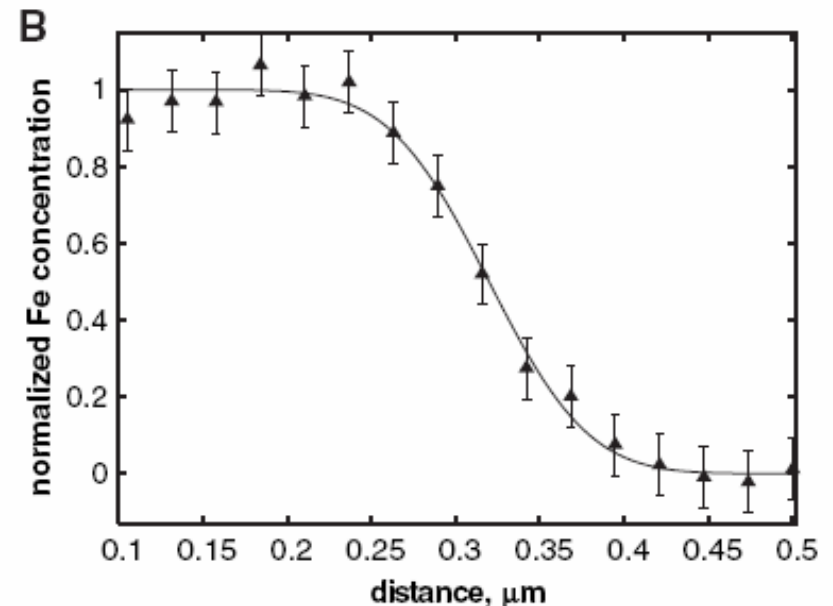
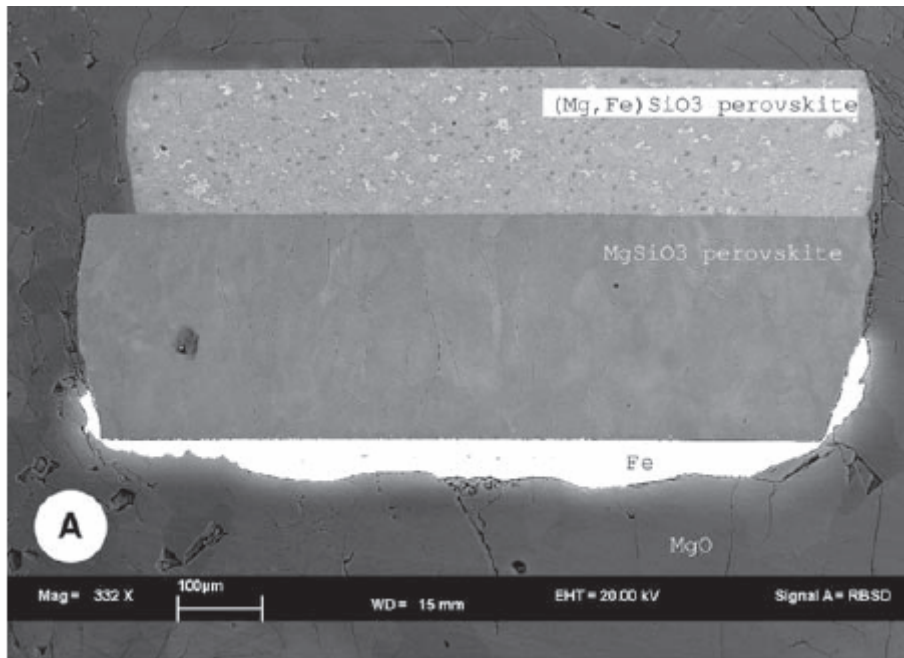
Kobayashi *et al*, *GRL* 2005

Murakami *et al*, *GRL* 2005

- Measurements on *P-T* quenched samples
- *In-situ* chemical probe

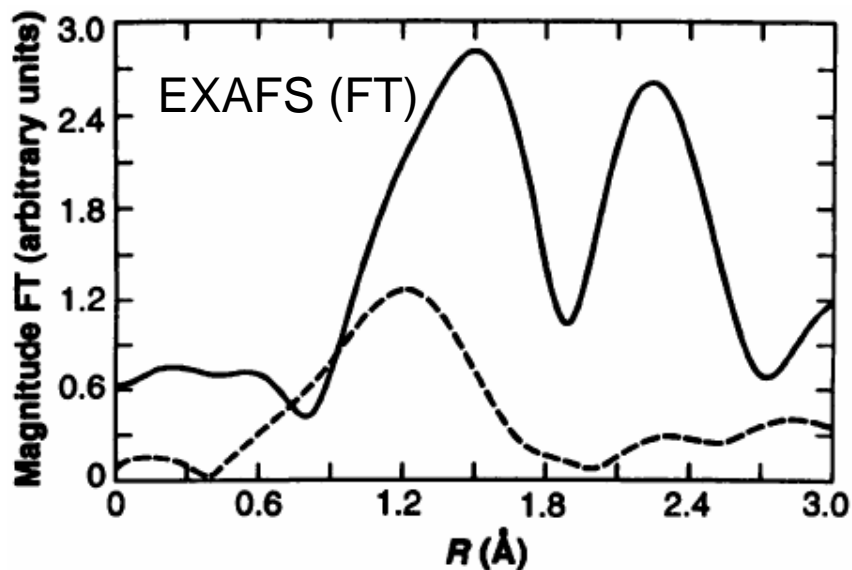
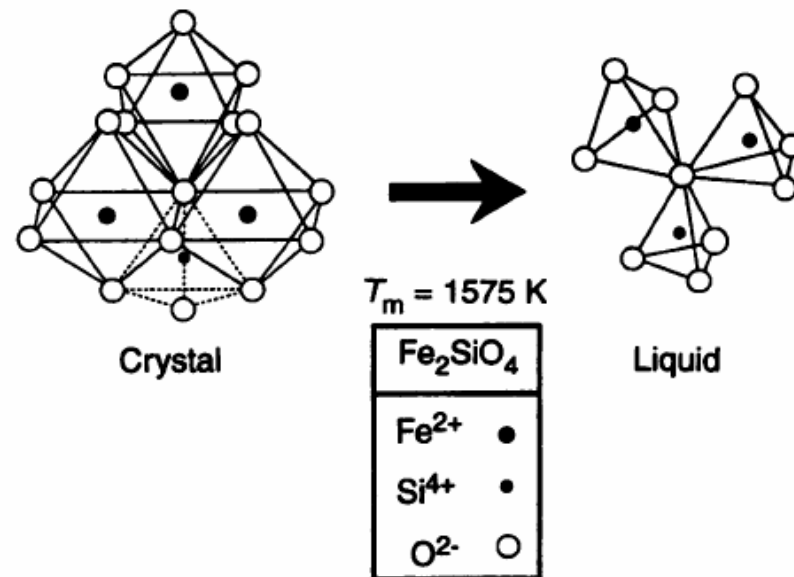
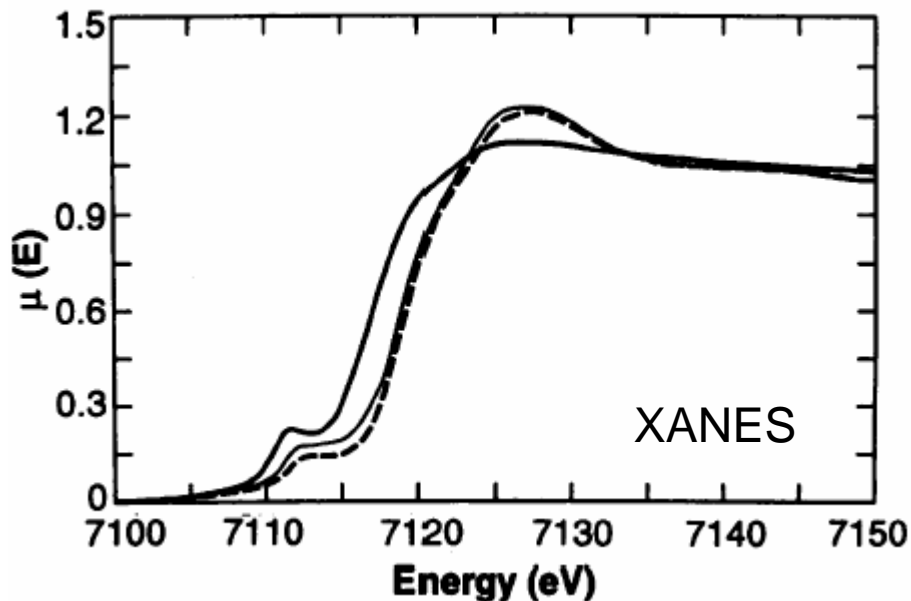
Fe-Mg diffusion

- Very sluggish Fe-Mg interdiffusion?
 - Chemical heterogeneities could persist several cycles of mantle convection (100 Ma)



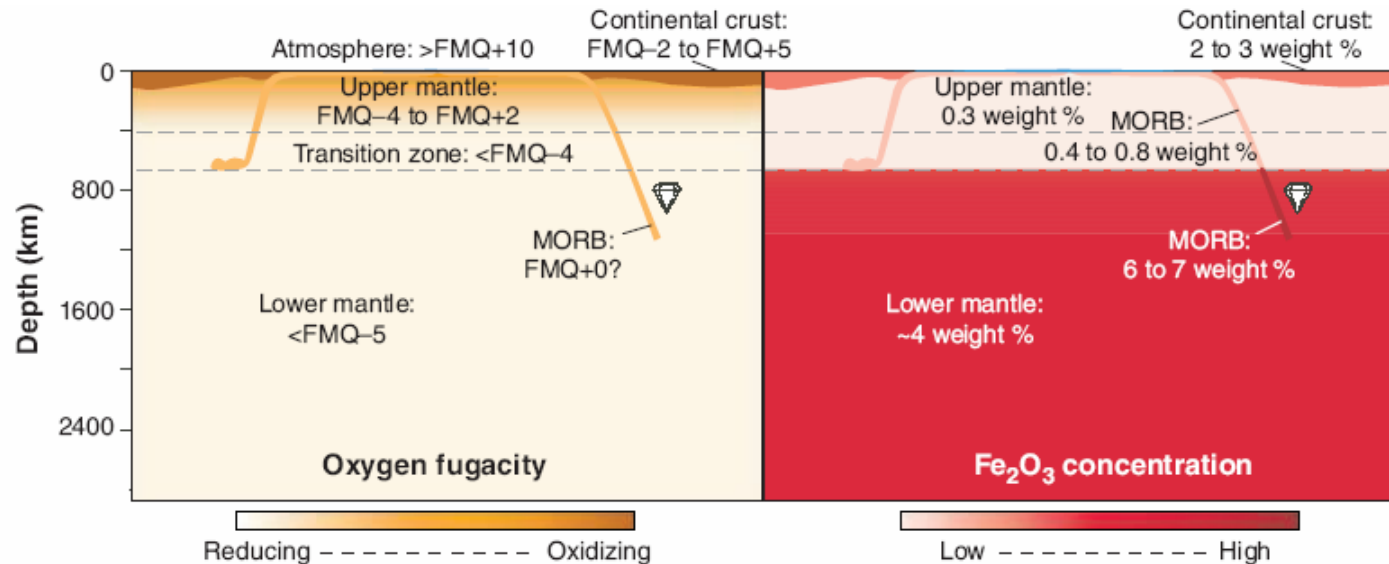
Holzapfel et al, *Science* 2005

Fe coordination in solid and liquid



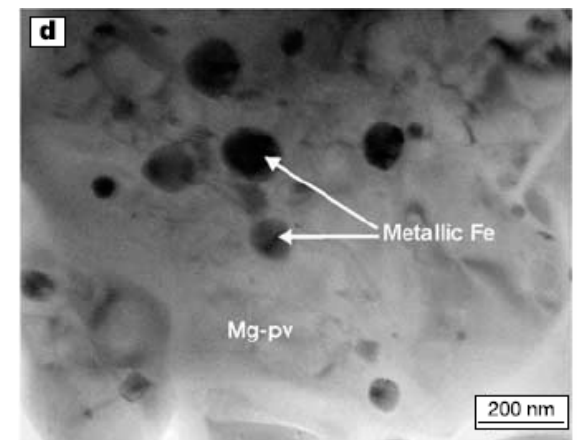
- 1 bar, HT experiment on fayalite (Fe_2SiO_4)
- $\text{VI Fe}^{2+}_{(\text{solid})} \rightarrow \text{IV Fe}^{2+}_{(\text{liq})}$

Fe redox



McCammon, Science 2005

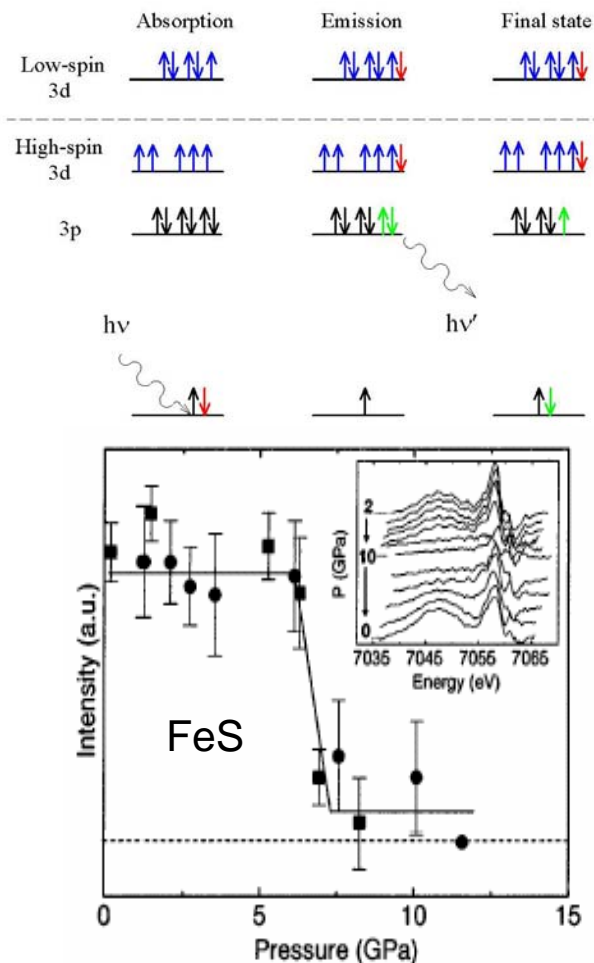
- Very high $\text{Fe}^{3+}/\Sigma\text{Fe}$ in LM?
 - 50% of Fe in pv (70 wt% of LM)
 - Inconsistent with whole-mantle convection (which would lead to similar oxygen content in UM and LM)
 - Oxygen could come from disproportionation of Fe^{2+} in LM, $3\text{Fe}^{2+} (3\text{FeO}) \rightarrow \text{Fe}^0 + 2\text{Fe}^{3+} (\text{Fe}_2\text{O}_3)$
 - LVP ~25 GPa, EELS and MS of quenched run product



Frost et al, Nature 2004

Electronic spin transitions

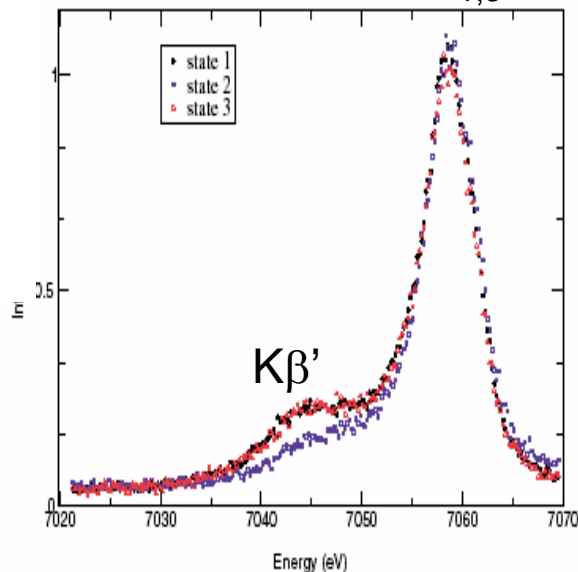
- Observations of high spin-low spin transitions in Fe using X-ray Emission Spectroscopy (XES)



Rueff et al. *PRL* 1999

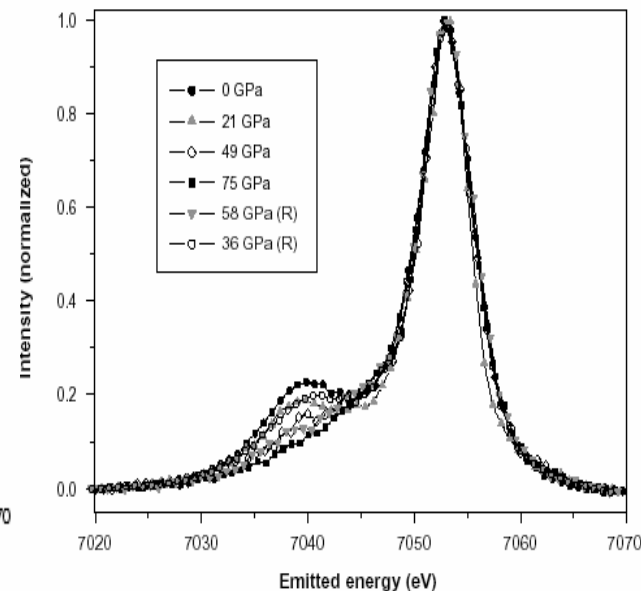
FeO & Fe₂O₃

K $\beta_{1,3}$



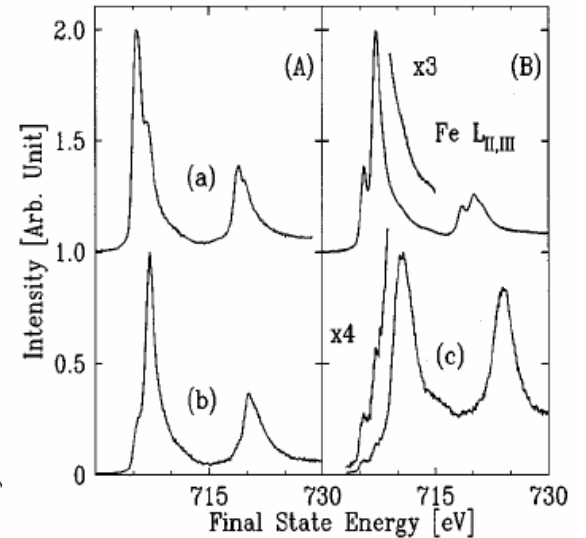
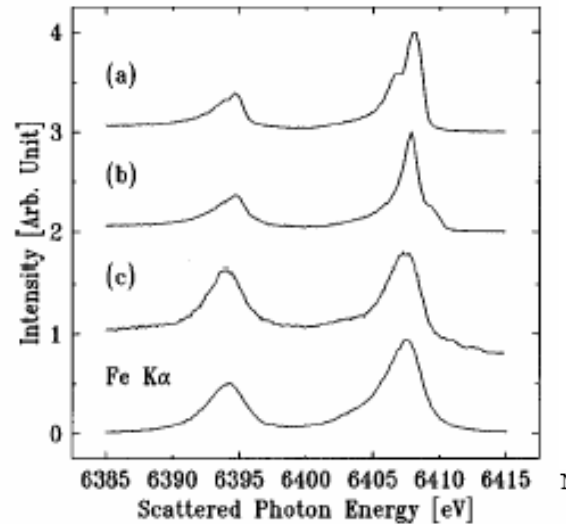
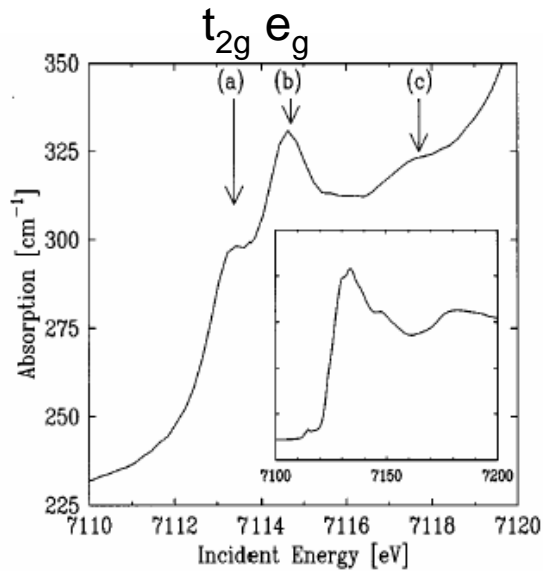
Badro et al, *PRL* 1999
Badro et al, *PRL* 2002

(Fe,Mg)O &
(Fe,Mg)SiO₃ pv



Badro et al, *Science* 2003
Badro et al, *Science* 2004
Li et al, *PNAS* 2004
Lin et al, *Nature* 2005
Lin et al, *Science* 2007

RXES



1s2p resonant inelastic x-ray scattering in α -Fe₂O₃

W. A. Caliebe,* C.-C. Kao, and J. B. Hastings

National Synchrotron Light Source, Brookhaven National Laboratory, Upton, New York, 11973

M. Taguchi[†] and A. Kotani

Institute for Solid State Physics, University of Tokyo, Roppongi, Minato-ku, Tokyo 106, Japan

T. Uozumi

College of Engineering, University of Osaka Prefecture, Gakuen-cho, Sakai 593, Japan

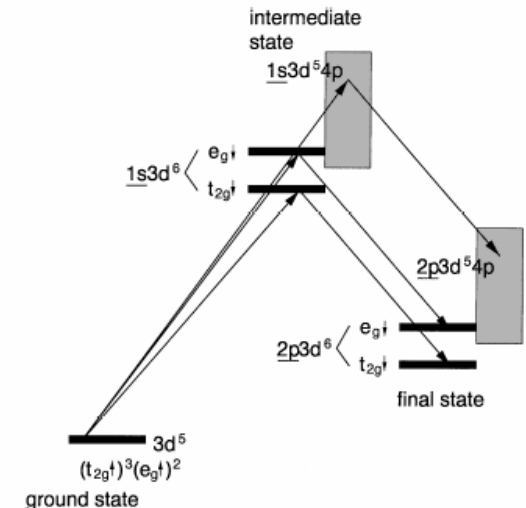
F. M. F. de Groot

Solid State Physics Laboratory, University of Groningen, Nijenborgh 4 9747 AG Groningen, The Netherlands

(Received 18 March 1998)

• X21 of NSLS

- Similar information to L_{2,3} absorption
- The pre-edge doublet due to crystal-field splitting



Fe in the deep Earth

- Our knowledge of Fe distribution relies on understanding the drastic changes in the physical and chemical properties of Fe species at extreme P - T conditions:
 - Fe/Mg partitioning
 - Fe/Mg diffusion
 - Fe speciation in solid and liquid
 - Mantle redox (ferric/ferrous)
 - Electronic spin state (high-intermediate-low)
- Progress in these areas have been dictated by advances in diagnostic high P - T probes (e.g. optical, Mössbauer, XRD, XES, and XAS)
- Extend these measurements to *in-situ* mantle P - T

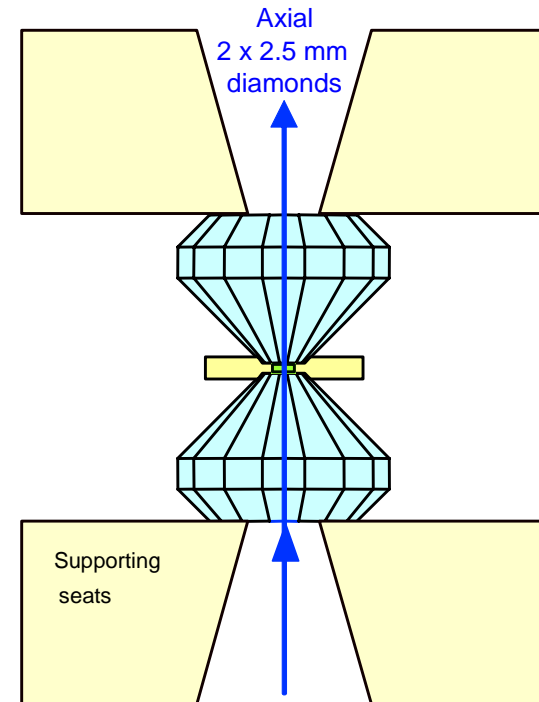
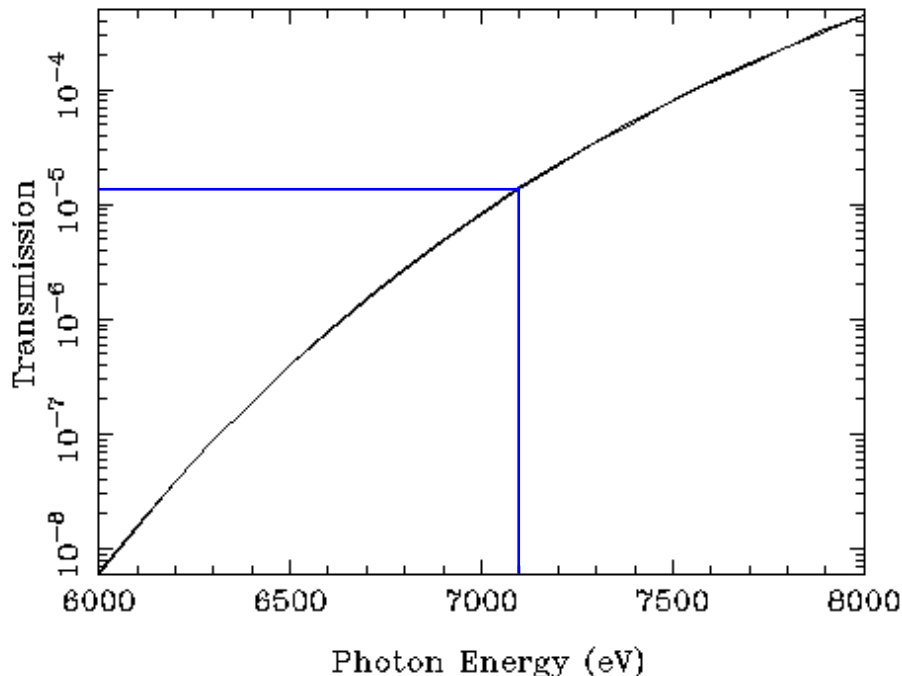
XAS in a DAC

- XAS has potential as a tool capable of answering all these questions, but has been hardly applied to high- P Fe studies due to the x-ray absorption of diamond anvils.
- Transmission of 7.1 keV x-ray at the Fe K -edge through a typical pair of diamond anvils (5 mm total thickness) is only 10^{-5} .

XAS in a DAC

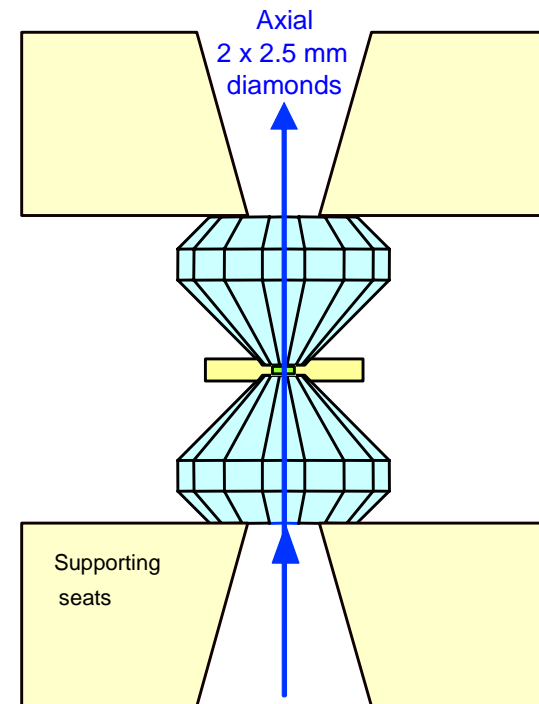
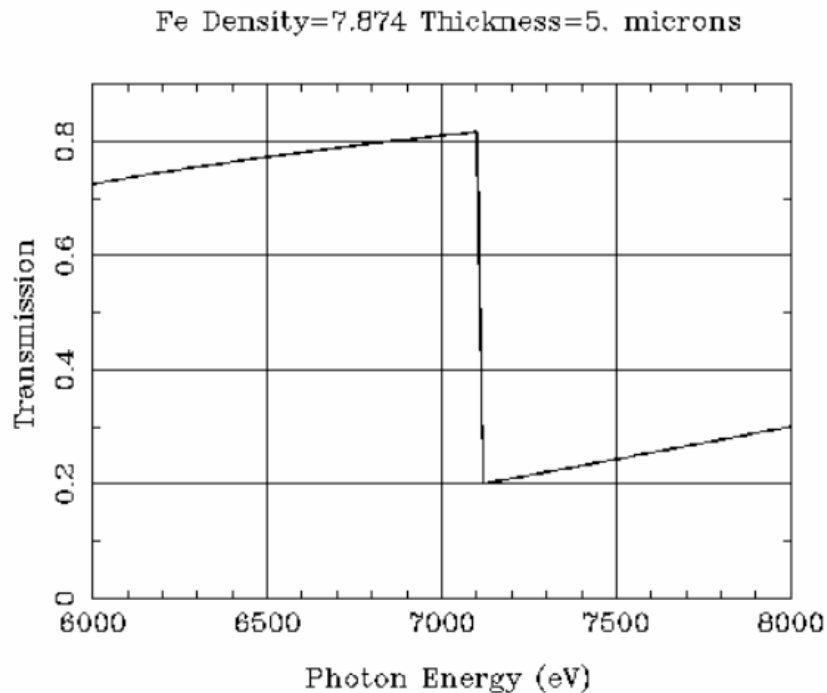
- XAS has potential as a tool capable of answering all these questions, but has been hardly applied to high- P Fe studies due to the x-ray absorption of diamond anvils.
- Transmission of 7.1 keV x-ray at the Fe K -edge through a typical pair of diamond anvils (5 mm total thickness) is only 10^{-5} .

C Density=3.5154 Thickness=5000. microns



XAS in a DAC

- XAS has potential as a tool capable of answering all these questions, but has been hardly applied to high- P Fe studies due to the x-ray absorption of diamond anvils.
- Transmission of 7.1 keV x-ray at the Fe K -edge through a typical pair of diamond anvils (5 mm total thickness) is only 10^{-5} .



XAS in a DAC

This problem has been overcome by:

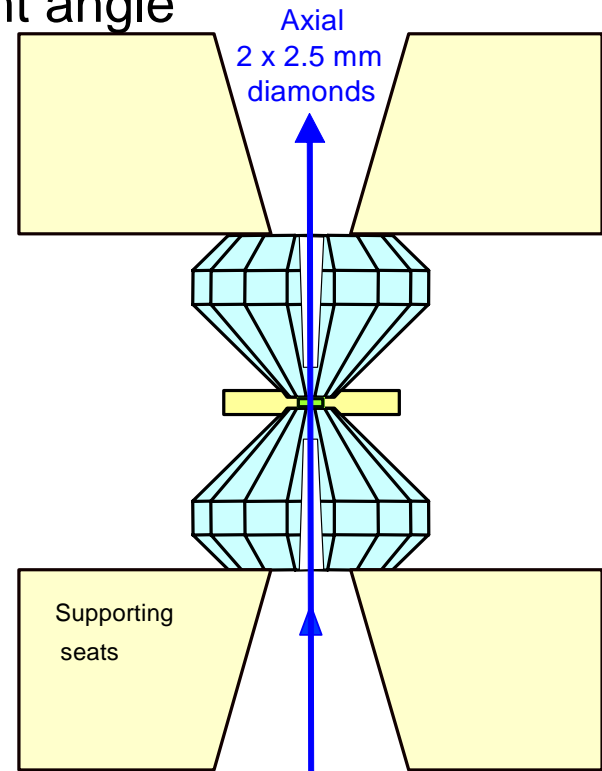
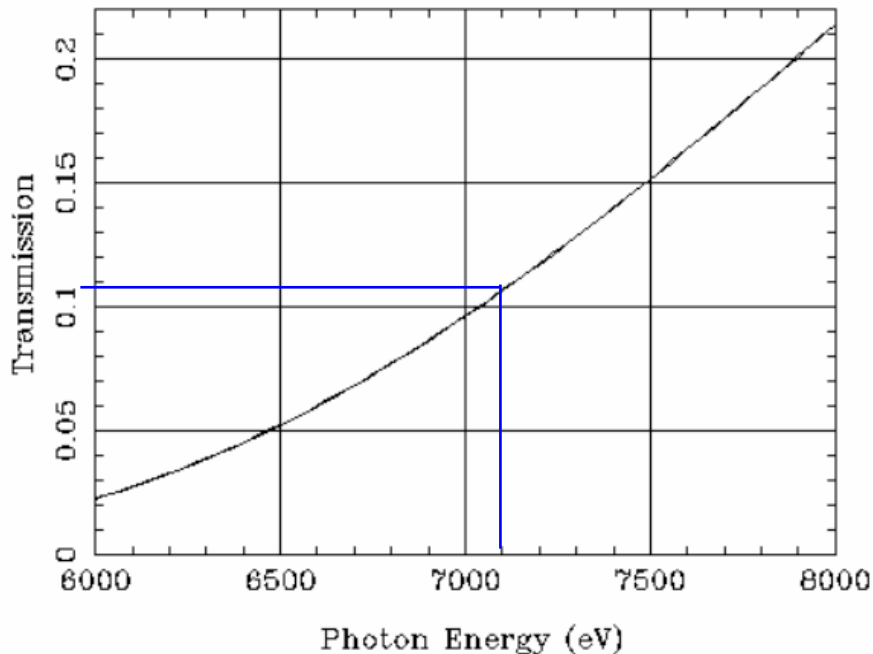
- Reducing the diamond thickness in the path down to 1 mm and transmission to a tolerable 0.1 by using holes in diamonds (Bassett et al., 2000; Dadashev et al., 2001)
- Supporting diamonds with holes (Silvera, 1999)
- Be gasket with inclined x-ray incident angle

XAS in a DAC

This problem has been overcome by:

- Reducing the diamond thickness in the path down to 1 mm and transmission to a tolerable 0.1 by using holes in diamonds (Bassett et al., 2000; Dadashev et al., 2001)
- Supporting diamonds with holes (Silvera, 1999)
- Be gasket with inclined x-ray incident angle

C Density=3.5154 Thickness=1000. microns

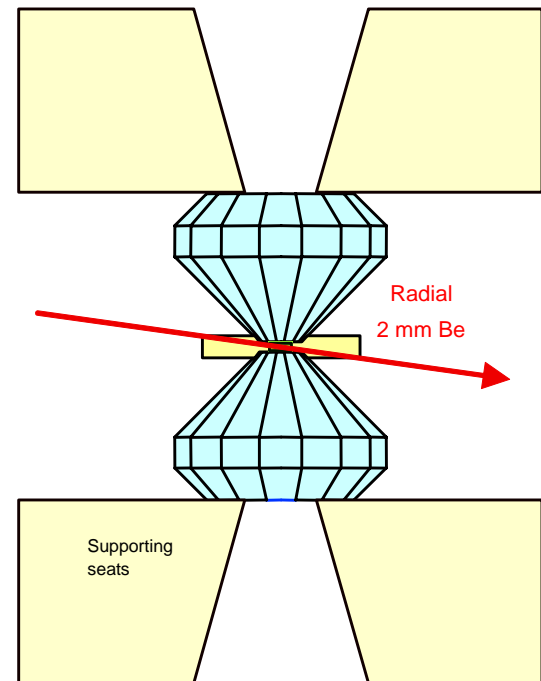
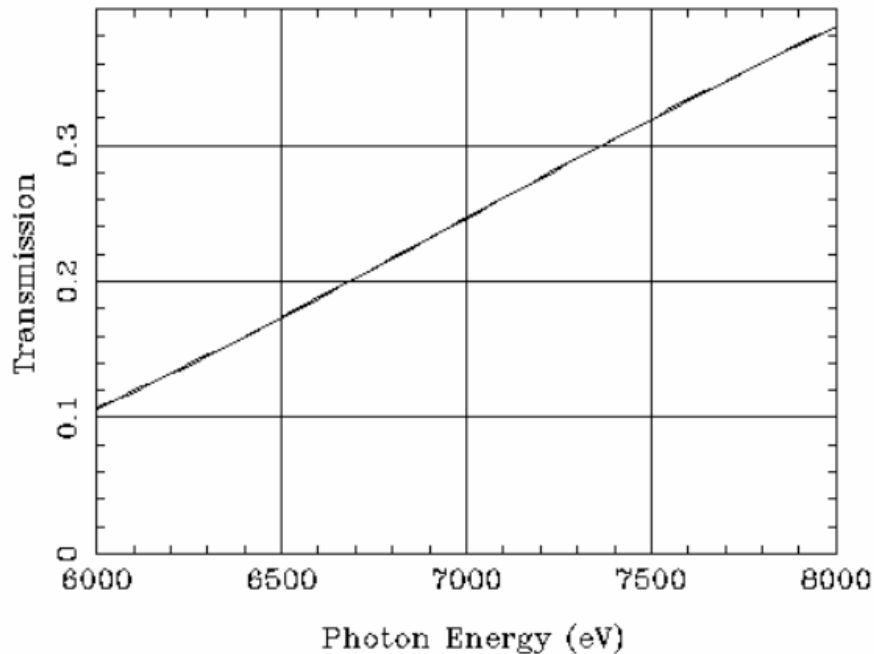


XAS in a DAC

This problem has been overcome by:

- Reducing the diamond thickness in the path down to 1 mm and transmission to a tolerable 0.1 by using holes in diamonds (Bassett et al., 2000; Dadashev et al., 2001)
- Supporting diamonds with holes (Silvera, 1999)
- Be gasket with inclined x-ray incident angle

Be Density=1.848 Thickness=5000. microns



XAS of Fe

- Pre-edge position and intensity – Fe oxidation state, coordination #, redox $\text{Fe}^{3+}/\Sigma\text{Fe}$
- Edge height: quantitative mapping of Fe
- CFSE of pre-edge 7113-7115 eV: $t_{2g}-e_g$
- XMCD: magnetism
- EXAFS: Fe coordination

1																	1	H	2	He															
3	Li	4	Be													5	B	6	C	7	N	8	O	9	F	10	Ne								
11	Na	12	Mg													13	Al	14	Si	15	P	16	S	17	Cl	18	Ar								
19	K	20	Ca	21	Sc	22	Ti	23	V	24	Cr	25	Mn	26	Fe	27	Co	28	Ni	29	Cu	30	Zn	31	Ga	32	Ge	33	As	34	Se	35	Br	36	Kr
37	Rb	38	Sr	39	Y	40	Zr	41	Nb	42	Mo	43	Tc	44	Ru	45	Rh	46	Pd	47	Ag	48	Cd	49	In	50	Sn	51	Sb	52	Te	53	I	54	Xe
55	Cs	56	Ba	57	La	72	Hf	73	Ta	74	W	75	Re	76	Os	77	Ir	78	Pt	79	Au	80	Hg	81	Tl	82	Pb	83	Bi	84	Po	85	At	86	Rn
87	Fr	88	Ra	89	Ac	104	Ru	105	Ha	106	Unh	107	Uns	108	Uno	109	Une																		

58	Ce	59	Pr	60	Nd	61	Pm	62	Sm	63	Eu	64	Gd	65	Tb	66	Dy	67	Ho	68	Er	69	Tm	70	Yb	71	Lu
90	Th	91	Pa	92	U	93	Np	94	Pu	95	Am	96	Cm	97	Bk	98	Cf	99	Es	100	Fm	101	Md	102	No	103	Lr

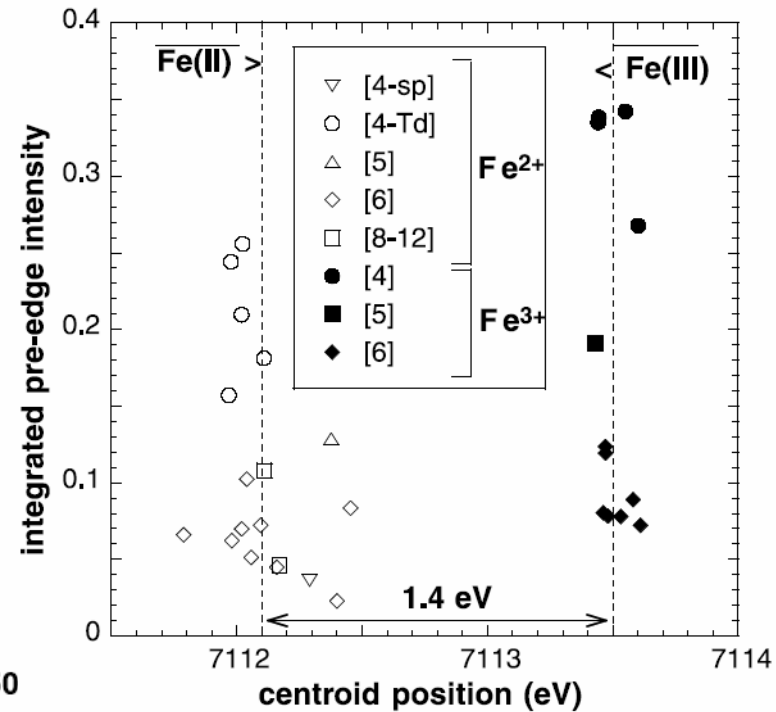
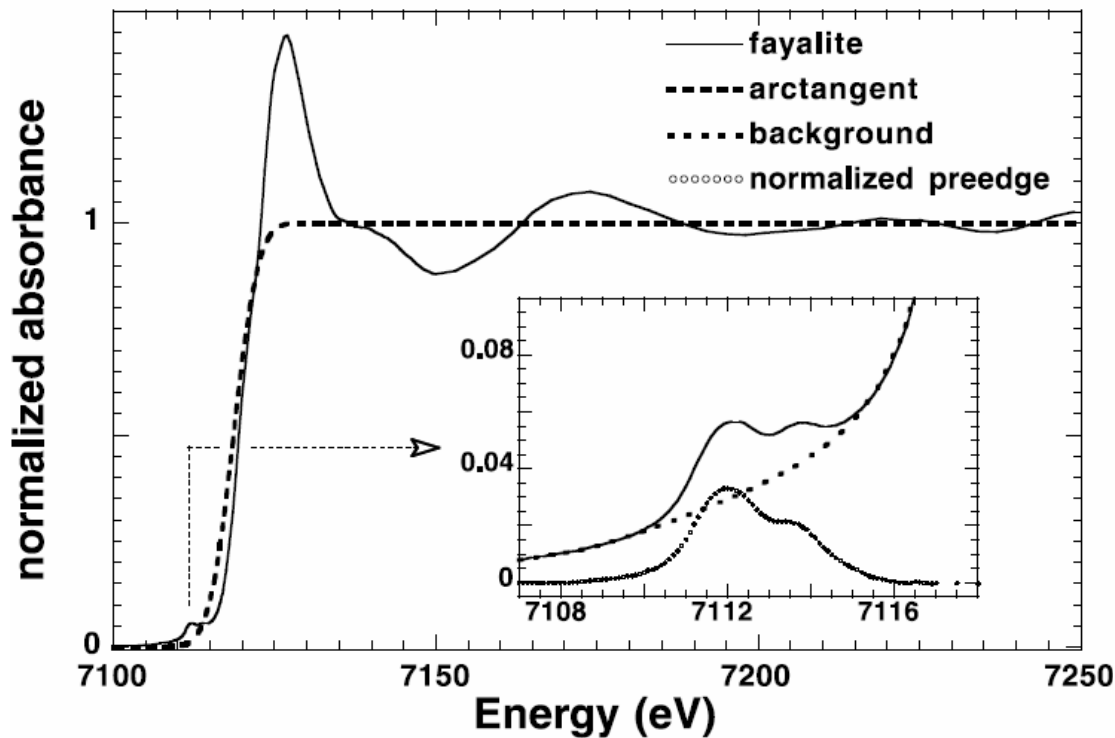
XAS of Fe

- Pre-edge position and intensity – Fe oxidation state, coordination #, redox $\text{Fe}^{3+}/\Sigma\text{Fe}$
- Edge height: quantitative mapping of Fe
- CFSE of pre-edge 7113-7115 eV: $t_{2g}-e_g$
- XMCD: magnetism
- EXAFS: Fe coordination

1																	1	2
H																	H	He
3	4											5	6	7	8	9	10	
Li	Be											B	C	N	O	F	Ne	
11	12											13	14	15	16	17	18	
Na	Mg											Al	Si	P	S	Cl	Ar	
19	20	21	22	23	24	25	26	27	28	29	30	31	32	33	34	35	36	
K	Ca	Sc	Ti	V	Cr	Mn	Fe	Co	Ni	Cu	Zn	Ga	Ge	As	Se	Br	Kr	
37	38	39	40	41	42	43	44	45	46	47	48	49	50	51	52	53	54	
Rb	Sr	Y	Zr	Nb	Mo	Tc	Ru	Rh	Pd	Ag	Cd	In	Sn	Sb	Te	I	Xe	
55	56	57	72	73	74	75	76	77	78	79	80	81	82	83	84	85	86	
Cs	Ba	La	Hf	Ta	W	Re	Os	Ir	Pt	Au	Hg	Tl	Pb	Bi	Po	At	Rn	
87	88	89	104	105	106	107	108	109										
Fr	Ra	Ac	Ru	Ha	Unh	Uns	Uno	Une										

58	59	60	61	62	63	64	65	66	67	68	69	70	71
Ce	Pr	Nd	Pm	Sm	Eu	Gd	Tb	Dy	Ho	Er	Tm	Yb	Lu
90	91	92	93	94	95	96	97	98	99	100	101	102	103
Th	Pa	U	Np	Pu	Am	Cm	Bk	Cf	Es	Fm	Md	No	Lr

Pre-edge position and intensity



- Redox and crystallographic site

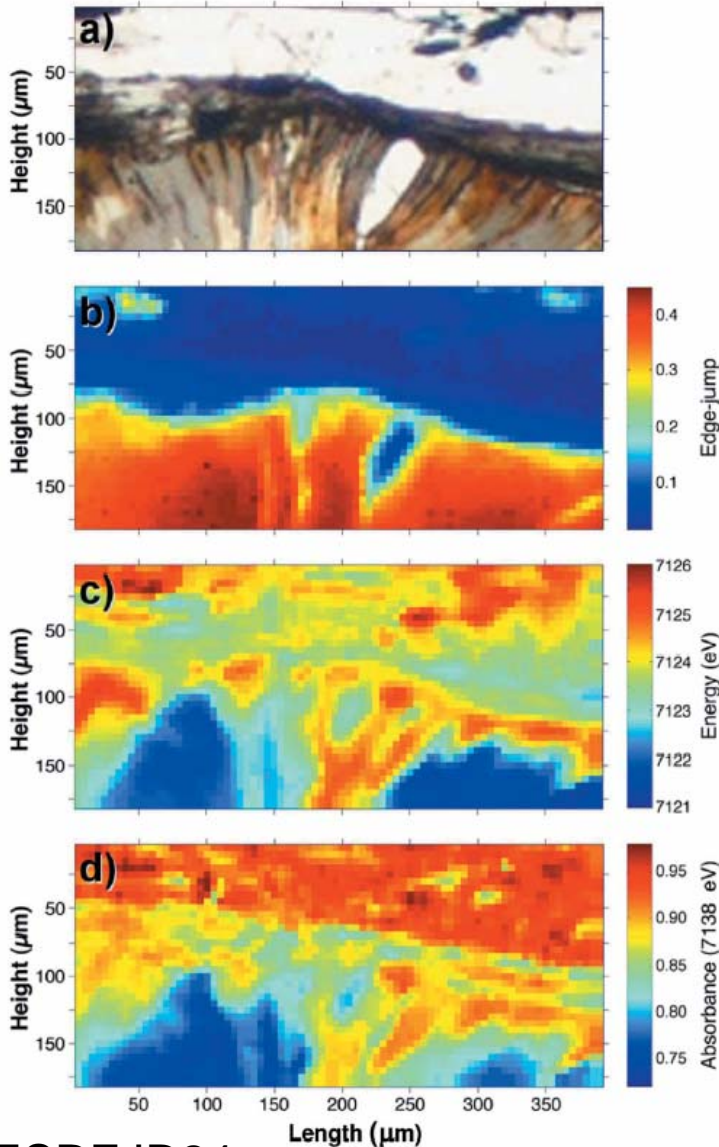
XAS of Fe

- Pre-edge position and intensity – Fe oxidation state, coordination #, redox $\text{Fe}^{3+}/\Sigma\text{Fe}$
- Edge height: quantitative mapping of Fe
- CFSE of pre-edge 7113-7115 eV: $t_{2g}-e_g$
- XMCD: magnetism
- EXAFS: Fe coordination

1																	1	2
H																	H	He
3	4											5	6	7	8	9	10	
Li	Be											B	C	N	O	F	Ne	
11	12											13	14	15	16	17	18	
Na	Mg											Al	Si	P	S	Cl	Ar	
19	20	21	22	23	24	25	26	27	28	29	30	31	32	33	34	35	36	
K	Ca	Sc	Ti	V	Cr	Mn	Fe	Co	Ni	Cu	Zn	Ga	Ge	As	Se	Br	Kr	
37	38	39	40	41	42	43	44	45	46	47	48	49	50	51	52	53	54	
Rb	Sr	Y	Zr	Nb	Mo	Tc	Ru	Rh	Pd	Ag	Cd	In	Sn	Sb	Te	I	Xe	
55	56	57	72	73	74	75	76	77	78	79	80	81	82	83	84	85	86	
Cs	Ba	La	Hf	Ta	W	Re	Os	Ir	Pt	Au	Hg	Tl	Pb	Bi	Po	At	Rn	
87	88	89	104	105	106	107	108	109										
Fr	Ra	Ac	Ru	Ha	Unh	Uns	Uno	Une										

58	59	60	61	62	63	64	65	66	67	68	69	70	71
Ce	Pr	Nd	Pm	Sm	Eu	Gd	Tb	Dy	Ho	Er	Tm	Yb	Lu
90	91	92	93	94	95	96	97	98	99	100	101	102	103
Th	Pa	U	Np	Pu	Am	Cm	Bk	Cf	Es	Fm	Md	No	Lr

Chemical mapping using micro-XAS



- ED-XAS
- Maps of:
 - Fe content
 - Redox
 - Crystallographic site

XAS of Fe

- Pre-edge position and intensity – Fe oxidation state, coordination #, redox $\text{Fe}^{3+}/\Sigma\text{Fe}$
- Edge height: quantitative mapping of Fe
- CFSE of pre-edge 7113-7115 eV: $t_{2g}-e_g$
- XMCD: magnetism
- EXAFS: Fe coordination

1																	1	2
H																	H	He
3	4											5	6	7	8	9	10	
Li	Be											B	C	N	O	F	Ne	
11	12											13	14	15	16	17	18	
Na	Mg											Al	Si	P	S	Cl	Ar	
19	20	21	22	23	24	25	26	27	28	29	30	31	32	33	34	35	36	
K	Ca	Sc	Ti	V	Cr	Mn	Fe	Co	Ni	Cu	Zn	Ga	Ge	As	Se	Br	Kr	
37	38	39	40	41	42	43	44	45	46	47	48	49	50	51	52	53	54	
Rb	Sr	Y	Zr	Nb	Mo	Tc	Ru	Rh	Pd	Ag	Cd	In	Sn	Sb	Te	I	Xe	
55	56	57	72	73	74	75	76	77	78	79	80	81	82	83	84	85	86	
Cs	Ba	La	Hf	Ta	W	Re	Os	Ir	Pt	Au	Hg	Tl	Pb	Bi	Po	At	Rn	
87	88	89	104	105	106	107	108	109										
Fr	Ra	Ac	Ru	Ha	Unh	Uns	Uno	Une										

58	59	60	61	62	63	64	65	66	67	68	69	70	71
Ce	Pr	Nd	Pm	Sm	Eu	Gd	Tb	Dy	Ho	Er	Tm	Yb	Lu
90	91	92	93	94	95	96	97	98	99	100	101	102	103
Th	Pa	U	Np	Pu	Am	Cm	Bk	Cf	Es	Fm	Md	No	Lr

High-spin to low-spin transition in hematite

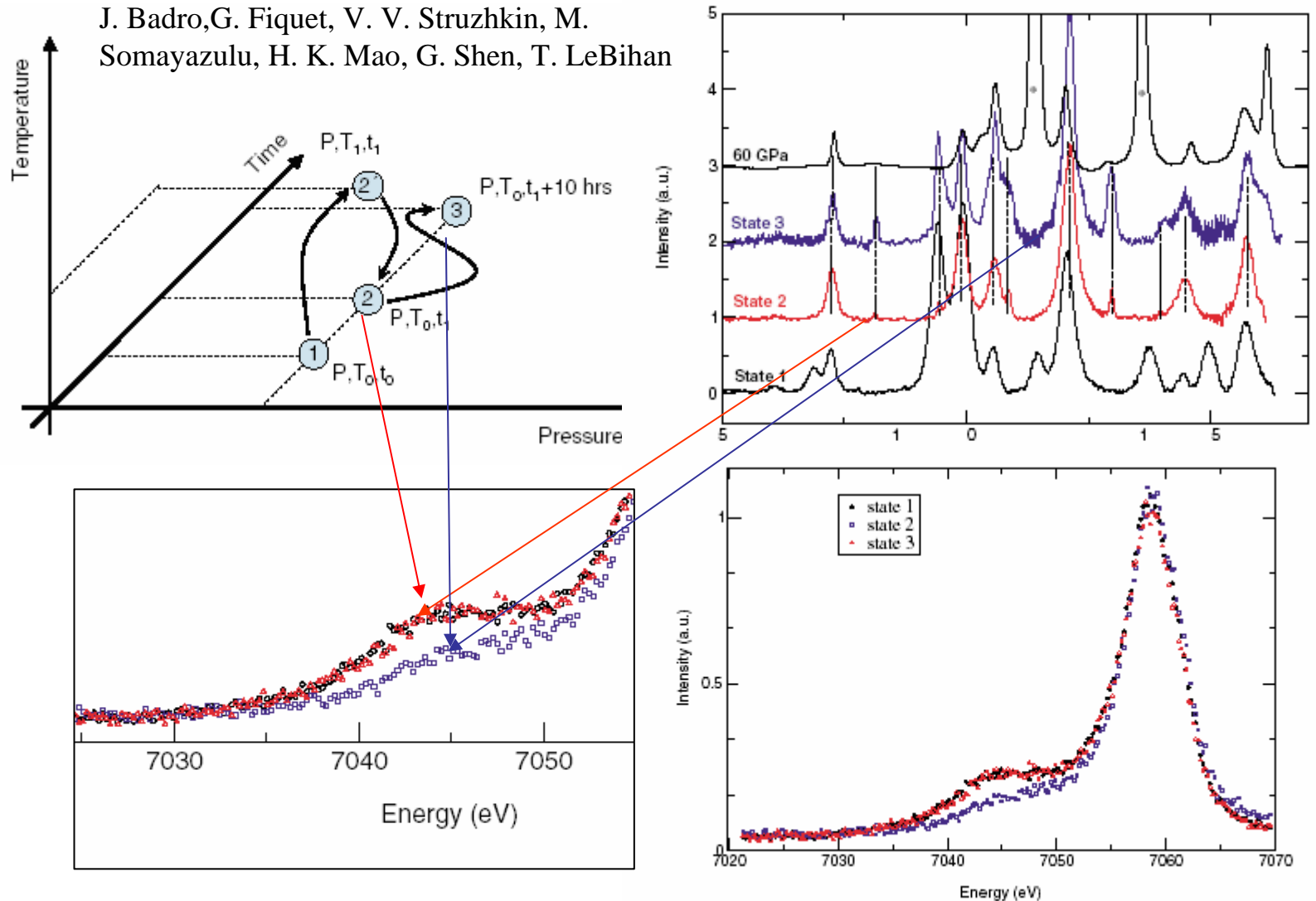
VOLUME 89, NUMBER 20

PHYSICAL REVIEW LETTERS

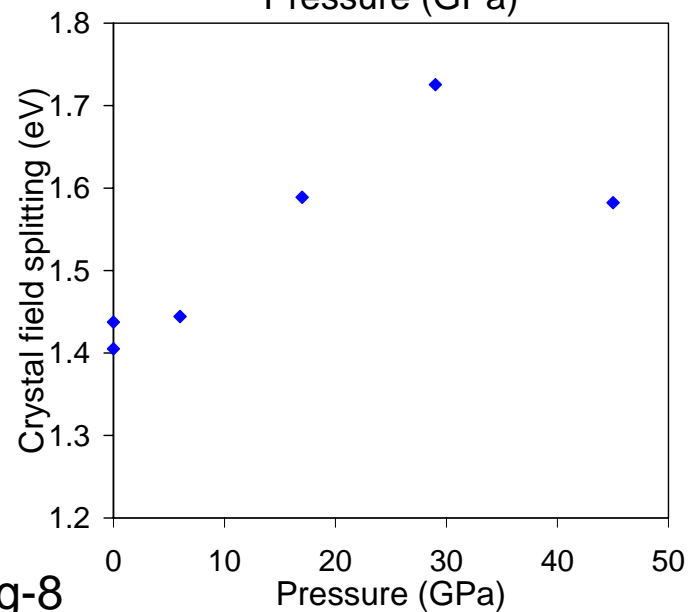
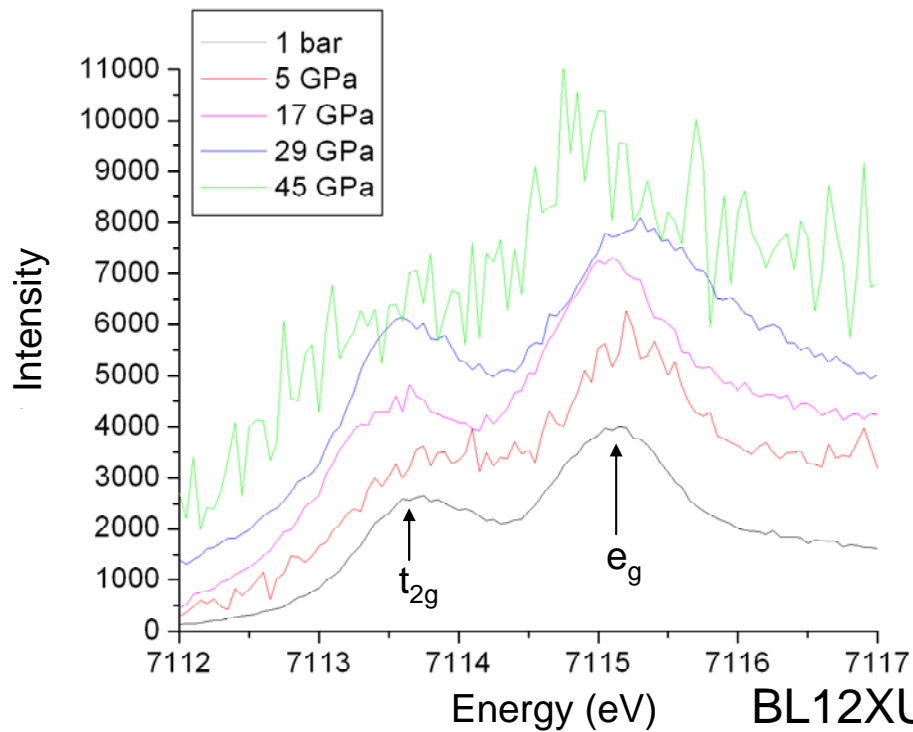
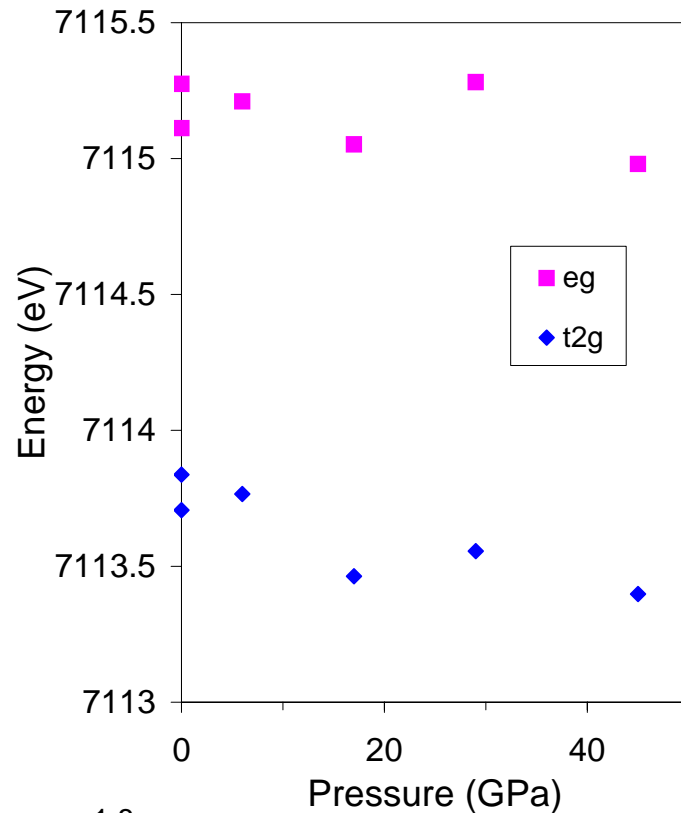
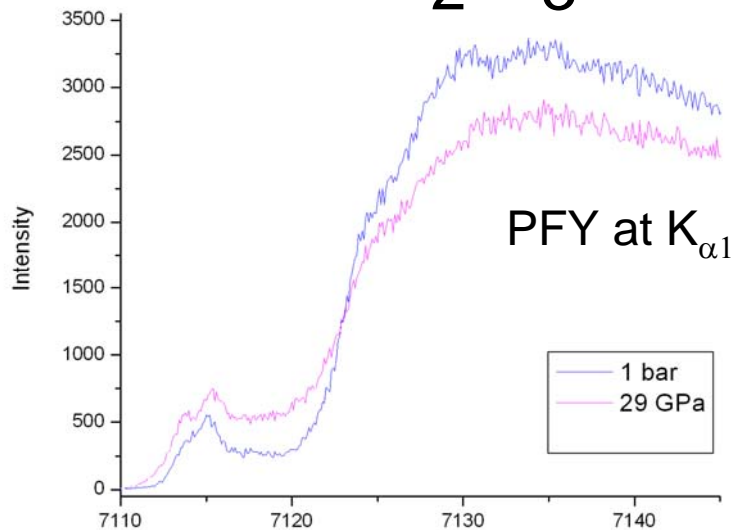
11 NOVEMBER 2002

Nature of the High-Pressure Transition in Fe_2O_3 Hematite

J. Badro, G. Fiquet, V. V. Struzhkin, M. Somayazulu, H. K. Mao, G. Shen, T. LeBihan



CFSE in Fe_2O_3



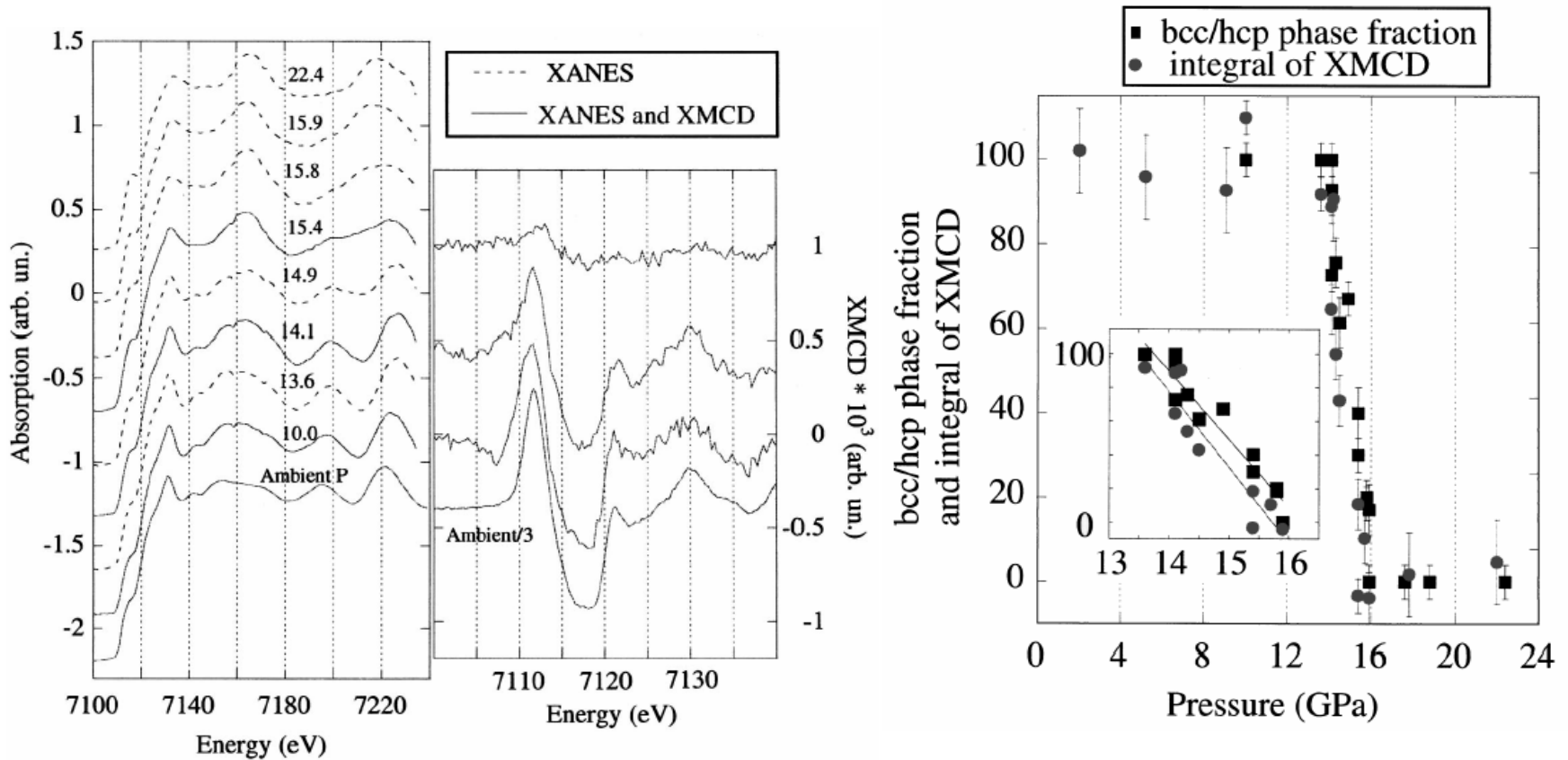
XAS of Fe

- Pre-edge position and intensity – Fe oxidation state, coordination #, redox $\text{Fe}^{3+}/\Sigma\text{Fe}$
- Edge height: quantitative mapping of Fe
- CFSE of pre-edge 7113-7115 eV: $t_{2g}-e_g$
- XMCD: magnetism
- EXAFS: Fe coordination

1																	1	2
H																	H	He
3	4											5	6	7	8	9	10	
Li	Be											B	C	N	O	F	Ne	
11	12											13	14	15	16	17	18	
Na	Mg											Al	Si	P	S	Cl	Ar	
19	20	21	22	23	24	25	26	27	28	29	30	31	32	33	34	35	36	
K	Ca	Sc	Ti	V	Cr	Mn	Fe	Co	Ni	Cu	Zn	Ga	Ge	As	Se	Br	Kr	
37	38	39	40	41	42	43	44	45	46	47	48	49	50	51	52	53	54	
Rb	Sr	Y	Zr	Nb	Mo	Tc	Ru	Rh	Pd	Ag	Cd	In	Sn	Sb	Te	I	Xe	
55	56	57	72	73	74	75	76	77	78	79	80	81	82	83	84	85	86	
Cs	Ba	La	Hf	Ta	W	Re	Os	Ir	Pt	Au	Hg	Tl	Pb	Bi	Po	At	Rn	
87	88	89	104	105	106	107	108	109										
Fr	Ra	Ac	Ru	Ha	Unh	Uns	Uno	Une										

58	59	60	61	62	63	64	65	66	67	68	69	70	71
Ce	Pr	Nd	Pm	Sm	Eu	Gd	Tb	Dy	Ho	Er	Tm	Yb	Lu
90	91	92	93	94	95	96	97	98	99	100	101	102	103
Th	Pa	U	Np	Pu	Am	Cm	Bk	Cf	Es	Fm	Md	No	Lr

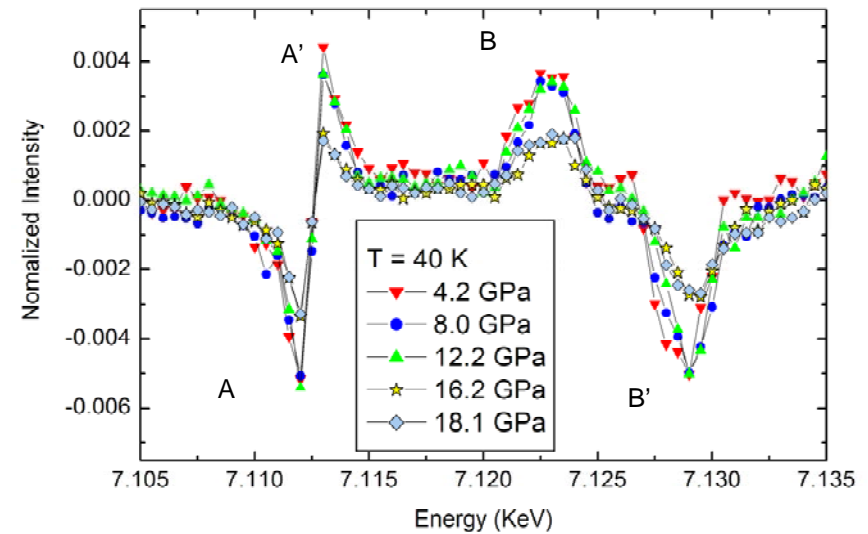
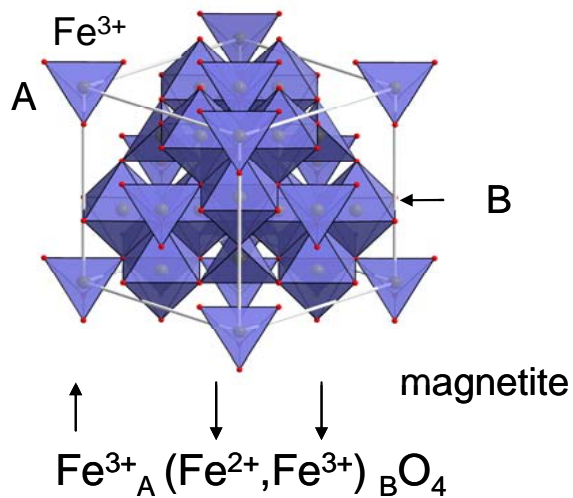
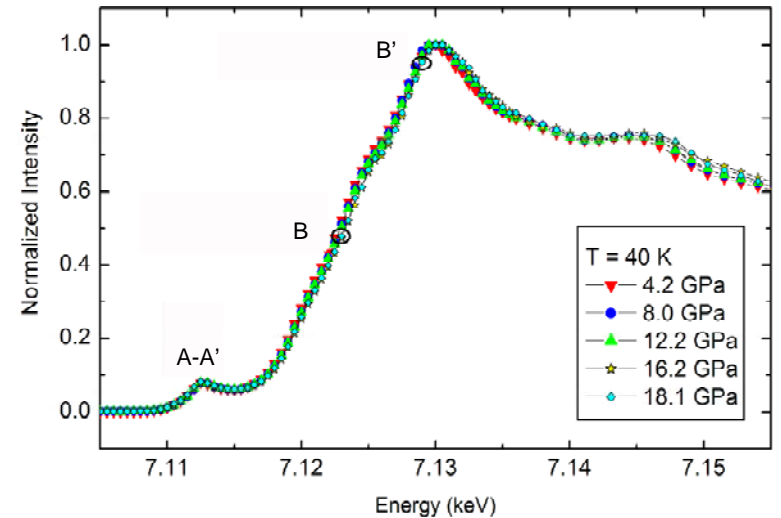
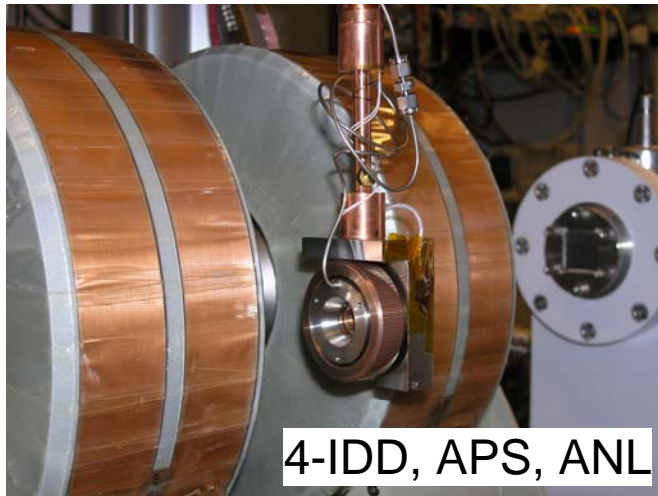
X-ray magnetic circular dichroism (XMCD) at HP



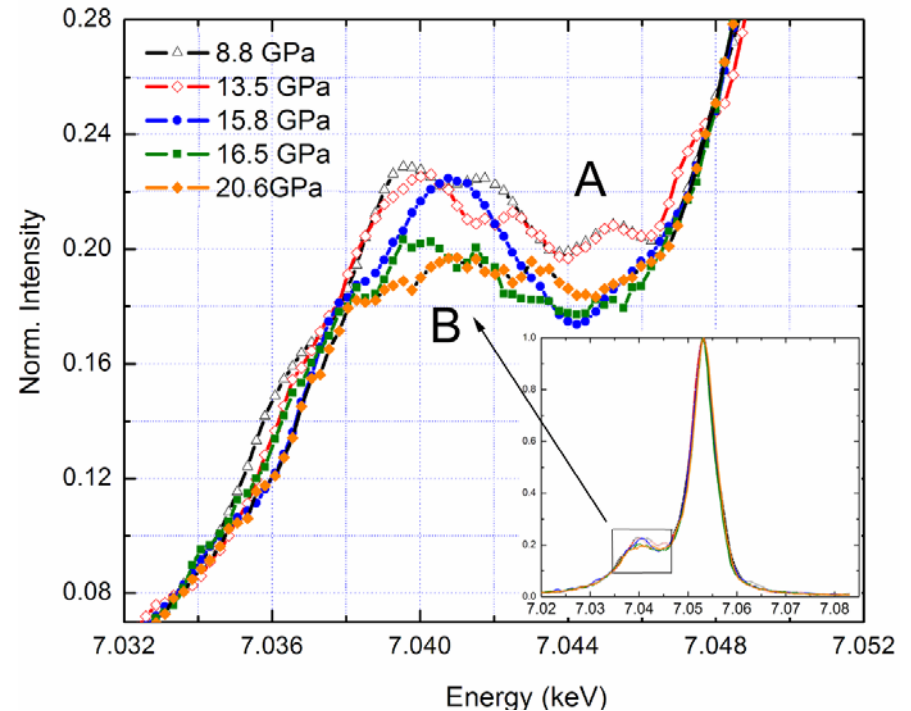
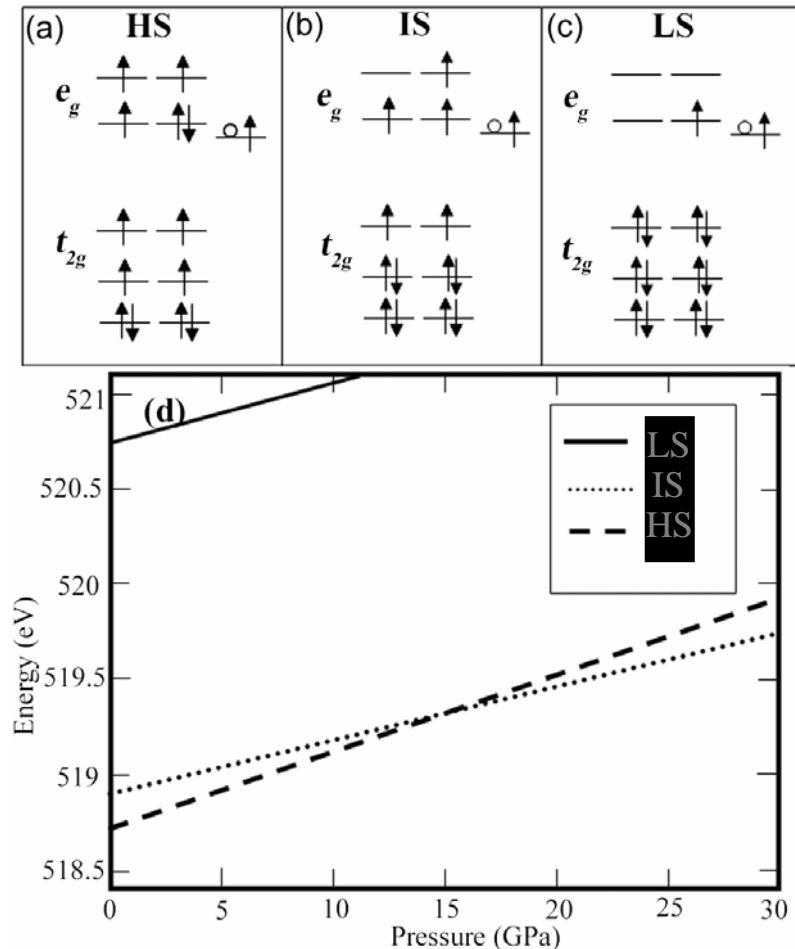
- bcc \rightarrow hcp transition in pure Fe
- Magnetic transition precedes (drives) structural

Mathon et al, *PRL* 2004

XMCD of Fe_3O_4 at HP



Intermediate spin in Fe²⁺



- Loss of 15% of intensity in K_{β}' peak
- Consistent with IS in Fe²⁺ and 2 Fe³⁺ remain HS

Multielectron energy levels of HS, IS, and low spin (LS) states of Fe²⁺ ion in FeO₆

Y. Ding et al, *PRL* in press

XAS of Fe

- Pre-edge position and intensity – Fe oxidation state, coordination #, redox $\text{Fe}^{3+}/\Sigma\text{Fe}$
- Edge height: quantitative mapping of Fe
- CFSE of pre-edge 7113-7115 eV: $t_{2g}-e_g$
- XMCD of near edge: magnetism
- EXAFS: Fe coordination

1																	1	2
H																	H	He
3	4											5	6	7	8	9	10	
Li	Be											B	C	N	O	F	Ne	
11	12											13	14	15	16	17	18	
Na	Mg											Al	Si	P	S	Cl	Ar	
19	20	21	22	23	24	25	26	27	28	29	30	31	32	33	34	35	36	
K	Ca	Sc	Ti	V	Cr	Mn	Fe	Co	Ni	Cu	Zn	Ga	Ge	As	Se	Br	Kr	
37	38	39	40	41	42	43	44	45	46	47	48	49	50	51	52	53	54	
Rb	Sr	Y	Zr	Nb	Mo	Tc	Ru	Rh	Pd	Ag	Cd	In	Sn	Sb	Te	I	Xe	
55	56	57	72	73	74	75	76	77	78	79	80	81	82	83	84	85	86	
Cs	Ba	La	Hf	Ta	W	Re	Os	Ir	Pt	Au	Hg	Tl	Pb	Bi	Po	At	Rn	
87	88	89	104	105	106	107	108	109										
Fr	Ra	Ac	Ru	Ha	Unh	Uns	Uno	Une										

58	59	60	61	62	63	64	65	66	67	68	69	70	71
Ce	Pr	Nd	Pm	Sm	Eu	Gd	Tb	Dy	Ho	Er	Tm	Yb	Lu
90	91	92	93	94	95	96	97	98	99	100	101	102	103
Th	Pa	U	Np	Pu	Am	Cm	Bk	Cf	Es	Fm	Md	No	Lr

Other topics to study

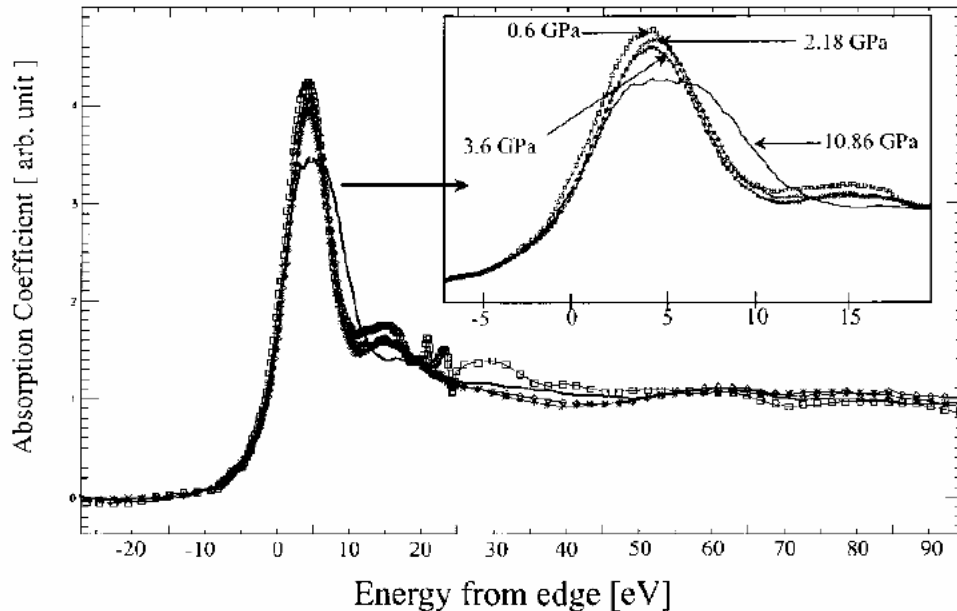
- Fe is just one example that shows the potential of high-pressure XAS in solving a wide range of scientific problems.
- These applications of high-pressure XAS can certainly be generalized to other elements including K-edge of TE and beyond and L-edge of REE and beyond, and have major impact in numerous other branches of high-pressure science.
- Its potential has been barely explored.
 - Absorption edge height – Quantitative mapping
 - Pre-edge and near edge features – oxidation states, electronic excitations
 - XMCD – magnetism
 - EXAFS – element specific structure of crystalline and amorphous materials

Absorption edge height

- Coupled with nanobeam capability, absorption edge height provides composition mapping and element specific tomography capability currently lacking in DAC experiments
- *In-situ* high pressure and temperature maps

Pre-edge and near edge

- Pressure has dramatic effects on charge transfer, mixed valence state, and oxidation state of d and f electron elements and compounds
- XAS can help to resolve various electronic states which are tuned by pressure



- HP behavior of X-ray near-edge structure at the rhenium L₃ edge in TlReO₄.
- No evidence for proposed e⁻ transfer from Tl to Re

Ablett et al, *HPR* 2003

XMCD

- Magnetism, MR (GMR and CMR), and spin character of lanthanides, manganites, cobaltites, etc.
- Pressure can readily tune these properties and change materials among many different magnetic and electronic states, providing opportunities for discovery and study of novel materials

PRL 97, 176405 (2006)

PHYSICAL REVIEW LETTERS

week ending
27 OCTOBER 2006

Spin State Transition in LaCoO_3 Studied Using Soft X-ray Absorption Spectroscopy and Magnetic Circular Dichroism

M. W. Haverkort,¹ Z. Hu,¹ J. C. Cezar,² T. Bumus,¹ H. Hartmann,¹ M. Reuther,¹ C. Zobel,¹ T. Lorenz,¹ A. Tanaka,³ N. B. Brookes,² H. H. Hsieh,^{4,5} H.-J. Lin,⁵ C. T. Chen,⁵ and L. H. Tjeng¹

PRL 98, 197203 (2007)

PHYSICAL REVIEW LETTERS

week ending
11 MAY 2007

Magnetism in Geometrically Frustrated YMnO_3 under Hydrostatic Pressure Studied with Muon Spin Relaxation

T. Lancaster,^{1,*} S. J. Blundell,¹ D. Andreica,^{2†} M. Janoschek,^{3,4} B. Roessli,⁴ S. N. Gvasaliya,⁴ K. Conder,⁵ E. Pomjakushina,^{4,5} M. L. Brooks,¹ P. J. Baker,¹ D. Prabhakaran,¹ W. Hayes,¹ and F. L. Pratt⁶

PRL 98, 137203 (2007)

PHYSICAL REVIEW LETTERS

week ending
30 MARCH 2007

Understanding the Insulating Phase in Colossal Magnetoresistance Manganites: Shortening of the Jahn-Teller Long-Bond across the Phase Diagram of $\text{La}_{1-x}\text{Ca}_x\text{MnO}_3$

E. S. Božin,¹ M. Schmidt,² A. J. DeConinck,¹ G. Paglia,¹ J. F. Mitchell,³ T. Chatterji,⁴ P. G. Radaelli,² Th. Proffen,⁵ and S. J. L. Billinge¹

Patterning of sodium ions and the control of electrons in sodium cobaltate

NATURE | Vol 445 | 8 February 2007

M. Roger¹, D. J. P. Morris², D. A. Tennant^{3,4}, M. J. Gutmann⁵, J. P. Goff², J.-U. Hoffmann³, R. Feyerherm³, E. Dudzik³, D. Prabhakaran⁶, A. T. Boothroyd⁶, N. Shannon⁷, B. Lake^{3,4} & P. P. Deen⁸

Lanthanide contraction and magnetism in the heavy rare earth elements

NATURE | Vol 446 | 5 April 2007

I. D. Hughes¹, M. Däne², A. Emst³, W. Hergert², M. Lüders⁴, J. Poulter⁵, J. B. Staunton¹, A. Svane⁶, Z. Szotek⁴ & W. M. Temmerman⁴



Exploring magnetism within extreme magnetic fields

last modified 07-01-2008 11:00

The feasibility of measuring X-ray magnetic circular dichroism (XMCD) within very high magnetic fields has been investigated using an energy-dispersive X-ray absorption spectrometer at the ESRF's energy-dispersive XAS beamline ID24.

By coupling a pulsed magnetic field device developed at the ESRF (**Figure 1**) [1] to the fast acquisition capabilities of ID24, the Re L_2 and L_3 XMCD signals were measured in a $\text{Ca}_2\text{FeReO}_6$ perovskite (**Figure 2**) at up to 30 T and in the temperature range 10-250 K [2]. Knowledge of the field and temperature dependence of both spin and orbital magnetic moments of Re under extreme magnetic fields could help answer enigmatic questions on the magnetism of these distorted double perovskites, such as why they don't reveal saturation, whether this phenomenon is only due to anisotropy in the grain boundaries or whether it originates from the bulk.

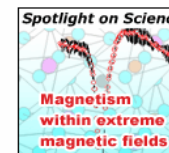
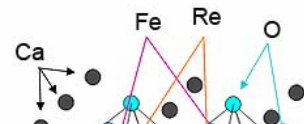


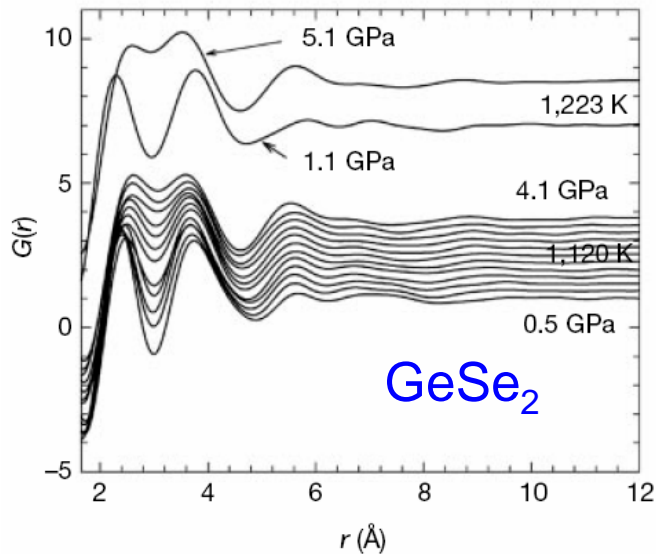
Figure 1: Peter van der Linden setting up the pulsed magnetic field device at beamline ID24.

Considerable research effort is being made to understand properties of matter under extreme conditions. Static high pressures up to the multimegabar regime can now be reached with diamond-anvil cells, as well as temperatures from the milli-Kelvin to thousands of Kelvin using dilution refrigerators and laser heating. The exploration of ever widening P-T diagrams has led to the discovery of a multitude of new chemical and physical phenomena - such as the discovery of the (Mg, Fe) SiO_3 postperovskite with significant geophysical implications for the earth mantle's nature and dynamics - leading to a fundamental understanding as well as technological applications.

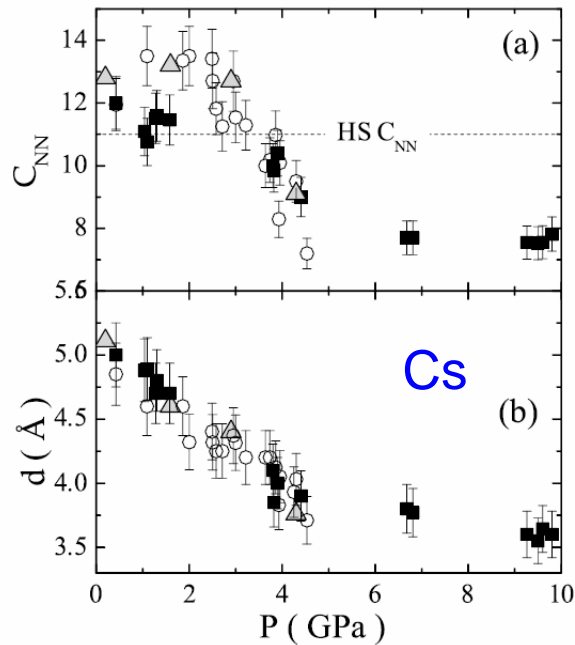


EXAFS

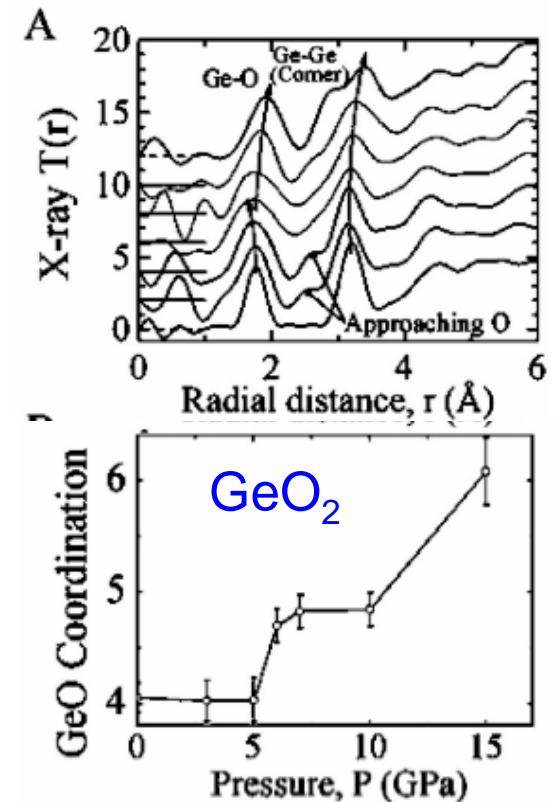
- Pressure induces polyamorphism in glasses and liquid-liquid transitions in high P - T melts. These transitions are normally observed by XRD
- EXAFS provide element specific coordination information



Crichton et al, *Nature* 2001



Falconi et al, *PRL* 2005



Guthrie et al, *PRL* 2004

Future opportunities enabled through NSLS II

- To optimize XAS capabilities would recommend design consideration of an integral system which can accommodate multiple extreme environments
 - High-pressure cells
 - Cryostat
 - Laser heating
 - Strong magnetic field